Digestive and Liver Disease 51 (2019) 1314–1322

Contents lists available at ScienceDirect

Digestive and Liver Disease

journal homepage: www.elsevier.com/locate/dld

Liver, Pancreas and Biliary Tract

MicroRNA-194 inhibits cell invasion and migration in hepatocellular carcinoma through PRC1-mediated inhibition of Wnt/β-catenin signaling pathway

Hui Tang [1], Hui Zhao [1], Zhen-Yu Yu, Xiao Feng, Bin-Sheng Fu, Chun-Hui Qiu *, Jian-Wen Zhang *

Department of Hepatic Surgery, Liver Transplantation Center, The Third Affiliated Hospital of Sun Yat-Sen University, Guangzhou, PR China

ARTICLE INFO

Article history:
Received 15 October 2018
Accepted 21 February 2019
Available online 1 March 2019

Keywords:
Epithelial-mesenchymal transition
Hepatocellular carcinoma
Invasion
MicroRNA-194
Migration
Protein regulator of cytokinesis 1
Wnt/β-catenin signaling pathway

ABSTRACT

Background: Hepatocellular carcinoma (HCC) is a commonly occurring malignancy accompanied by significant mortality rates. More recently, extensive investigations into microRNA (miRNA) expression profiles have been conducted to identify their ability to inhibit tumors. Thus, this study explored the role of miR-194 in epithelial-mesenchymal transition (EMT), cell invasion and migration through Wnt/β-catenin signaling pathway by binding to protein regulator of cytokinesis 1 (PRC1) in HCC.
Methods: Initially, HCC related microarray data were retrieved and analyzed, and regulatory miRNAs of PRC1 were predicted accordingly. Next, the roles of miR-194, PRC1, and Wnt/β-catenin signaling pathway in HCC were determined, with relationship between PRC1 and miR-194 being verified subsequently. The role of miR-194 in cell EMT, migration, proliferation and invasion was evaluated through gain- and loss-function studies. Finally, tumor xenograft in nude mice was induced to assess tumor growth of HCC.
Results: miR-194 affected HCC development in Wnt/β-catenin signaling pathway with putative binding sites to PRC1. MiR-194 could target PRC1. MiR-194 was downregulated while PRC1 was upregulated in HCC tissues. Additionally, miR-194 elevation and PRC1 silencing could suppress EMT, growth, proliferation, invasion, and migration in HCC cells by inactivating Wnt/β-catenin signaling pathway.
Conclusion: Taken together, this study demonstrated that miR-194 inhibited EMT, cell invasion and migration through inactivation of PRC1-dependent Wnt/β-catenin signaling pathway.

1. Introduction

With over half a million new cases diagnosed worldwide every year, hepatocellular carcinoma (HCC) is regarded as the fifth most commonly occurring tumor in the male population and seventh among their female counterparts [1]. The pathogenesis of HCC includes complex interactions of the abnormal activated signaling pathways, infection of hepatitis B virus, environmental and genetic factors [2,3]. During its early stages, HCC can be treated effectively by liver transplantation, locoregional treatments and surgical excision, and targeted molecular therapies have been speculated to be capable of providing improved outcome for HCC patients at more advanced stages [4]. Accumulating reports have highlighted the potential of microRNAs (miRNAs) for future cancer therapy [5]. Although improved treatment approaches have been achieved over the past few years, patients suffering from HCC are still faced with a high risk of mortality due to the poor prognosis, postoperative recurrence and metastasis associated with HCC, in addition to primary tumor occurrence and progression [6,7] thus highlighting the urgent need to identify novel targets for the diagnosis and treatment of HCC.

MiRNAs are small (approximately 22 nt), endogenous, non-coding RNA molecules that have been linked with the inhibition of gene expression at post-transcriptional level in a suppressive, degrading, or transferring fashion, and their abnormal expression has been detected in a wide variety of cancers [8]. Besides, evidence has indicated the key regulatory roles of miRNAs in the process of gene expression, with ability to influence almost the whole field of cell biology [9]. A recent study has demonstrated that tumor cell

* Corresponding authors at: Department of Hepatic Surgery, Liver Transplantation Center, The Third Affiliated Hospital of Sun Yat-Sen University, No. 600, Tianhe Road, Tianhe District, Guangzhou 510630, Guangdong Province, PR China
E-mail addresses: henryqiu@163.com (C.-H. Qiu), zhjianw2@mail.sysu.edu.cn (J.-W. Zhang).
[1] These authors contributed equally to this work.

https://doi.org/10.1016/j.dld.2019.02.012
1590-8658/

development is inhibited by miR-361-5p by binding to CXCR6 in HCC [10]. The expression of miR-194 has long been explored in the liver, with evidence presented highlighting its promise as a hepatic epithelial cell biomarker capable of inhibiting cell metastasis in HCC mice [11]. In the present study, bioinformatics prediction and dual luciferase reporter assay were employed in order to verify the putative binding sites between miR-194 and the 3'untranslated regions (UTR) of protein regulator of cytokinesis 1 (PRC1). PRC1 is a protein associated with microtubules and plays a distinct role in microtubules tissue and cytokinesis [12]. Moreover, the knockdown of PRC1 has been shown to inhibit bladder and breast cancer cell growth and proliferation, which provides new insights for novel anti-cancer therapies [13]. Additionally, PRC1 plays an oncogenic role in enhancing tumor formation, transfer, stemness and development of early HCC through the Wnt/β-catenin signaling pathway [14]. The Wnt/β-catenin signaling pathway is an important regulator in tumor formation and the size of organ, as well as tissue homeostasis [15]. Meanwhile, this signaling pathway has been strongly linked with liver zonation, regeneration, and progression and its abnormal activation has been manifested in cancers [16]. A recent study has demonstrated that the Wnt/β-catenin signaling pathway may function as a therapeutic target in the treatment of HCC patients [17]. In addition, HCC cell progression is suppressed by destruxin B through regulating epithelial-mesenchymal transition (EMT) and inactivation of the Wnt/β-catenin signaling pathway [18]. Therefore, the central objective of the present study was to investigate the underlying molecular mechanisms of miR-194, PRC1 and the Wnt/β-catenin signaling pathway in HCC with the hope of providing a fresh perspective in the search for new therapeutic strategies for HCC patients.

2. Materials and methods

2.1. Ethics statement

The study was approved by the Institutional Review Board of the Third Affiliated Hospital of Sun Yat-Sen University and was performed in strict accordance with the *Declaration of Helsinki*. Written informed consent documentation was obtained from each participant.

2.2. Microarray-based analysis

HCC expression profiles were retrieved and downloaded from the Gene Expression Omnibus (GEO) database (https://www.ncbi.nlm.nih.gov/geo/). The limma package in the R Programming Language was utilized for differential expression analysis with the p value < 0.05 and |LogFold Change| >2 as the screening threshold of differentially expressed genes (DEGs). The heat map package was employed in the construction of heat maps for DEGs. A Venn diagrams online construction website (http://bioinformatics.psb.ugent.be/webtools/Venn/) was applied in order to obtain the intersections of the three expression profiles. Cancer database of the Kyoto Encyclopedia of Genes and Genomes (KEGG) (http://www.kegg.jp/kegg/disease/cancer.html) was applied to obtain the known genes related with HCC. Besides, the Search Tool for the Retrieval of Interacting Genes/Proteins (STRING) database (https://string-db.org/) was utilized for correlation analysis between the DEGs and the known genes. Moreover, a gene interaction network was constructed using Cytoscape software. StarBase database (http://starbase.sysu.edu.cn/), miRSearch database (https://www.exiqon.com/miRSearch), miRNApath database (http://lgmb.fmrp.usp.br/mirnapath/tools.php), mirDIP database (http://ophid.utoronto.ca/mirDIP/index.jsp#r) and TargetScan database (http://www.targetscan.org/vert_71/) were all used to predict the regulatory miRNAs of PRC1 and identify the intersection of the predicted results.

2.3. Study subjects

For 4 years, March 2012 to March 2016, 228 HCC tissues were resected from patients diagnosed with primary HCC at the Third Affiliated Hospital of Sun Yat-Sen University. None of those patients received chemoradiotherapy prior to the operation. The adjacent normal tissues from the same patients were regarded as the normal control. The patients consisted of 157 males and 71 females (aged 35–69 years, with a mean age of 51.2 ± 17.6 years), among which 176 patients were confirmed with a history of hepatitis B infection, 12 patients with a history of hepatitis C infection and 8 patients with a history of both hepatitis B and hepatitis C infection. According to the Edmondson tumor pathological grading [19], 145 patients were classified as grades I to II and 83 patients were classified as grades II to IV. According to the Union for International Cancer Control (UICC) on tumor-nodes-metastasis (TNM) classification [20], 158 patients were confirmed to be at stages I to II, and 70 patients were noted to be at stages III to IV. Patients were included in the study based on the following criteria: (A) the patients who were pathologically diagnosed with primary HCC; (B) the patients who had complete clinical data; (C) the patients who did not have a history of chemotherapy or radiotherapy treatment. All patients were excluded from the current study in the event that: (A) the patients who had not received treatment at the Third Affiliated Hospital of Sun Yat-Sen University after diagnosis; (B) the patients who received treatment at any other hospitals; (C) the patients who had been pathologically diagnosed with carcinoma in situ; (D) the patients who had other malignancies. The tissue samples were collected from the aforementioned 228 HCC patients and promptly washed with normal saline. Next, the central parts of the HCC tissues and the adjacent normal tissues (5 cm away from the HCC tissues) were collected, placed in a respective manner into the frozen pipe and quickly cryopreserved in a liquid nitrogen container at −196 °C. This process must be finished within 10 min. After being sent to the laboratory, the samples were preserved at −80 °C.

2.4. Immunohistochemistry

All the tissue samples were fixed in 10% neutral formalin, embedded in paraffin, and sliced into 4-μm slices. The slices were then incubated in an incubator at 60 °C for 1 h, dewaxed into three cylinders containing xylene for 30 min (10 min per cylinder), dehydrated using gradient alcohol (100%, 95%, 75%, 1 min each) and washed under running water for 1 min. The slices were then incubated with 3% H_2O_2 (84885, Sigma-Aldrich, St Louis, Missouri, USA) at 37 °C for 30 min in order to block endogenous peroxidase. After phosphate buffer saline (PBS) washing for 3 min, the slices were subsequently added with 0.01 M citric acid buffer, boiled at 95 °C for 20 min, cooled to room temperature and sealed with normal goat serum working solution at 37 °C for 10 min. After this, primary antibody rabbit anti-mouse polyclonal antibody PRC1 (1: 10000, ab51248, Abcam Inc., Cambridge, MA, UK) was used to incubate the slices at 4 °C overnight. Subsequently, the slices were incubated with horseradish peroxidase (HRP)-labeled goat-anti-mouse immunoglobulin G (IgG) antibody (1: 10000, ab6789, Abcam Inc., Cambridge, MA, UK) at room temperature for 30 min. Then, the slices were visualized with diaminobenzidine (DAB) (ab64238, Abcam Inc., Cambridge, MA, USA), counterstained with hematoxylin and mounted. The PBS served as negative control (NC) instead of the primary antibody. Five high-power fields (200×, 100 cells per field) were selected randomly from each slice. The scores were determined based on the percentage of positive cells [21].

2.5. HCC cell line selection

Human normal hepatocyte L02 was purchased from Shanghai Xin Yu Biotech Co., Ltd (Shanghai, China). The HCC cells lines (HepG2, Hep 3B2.1-7, Huh-7 and Li-7) were purchased from the Cell Bank in Shanghai cell biology institute of Chinese Academy of Sciences (Shanghai, China). The above cells were incubated in a Roswell Park Memorial Institute (RPMI) 1640 medium (Gibco Company, Grand Island, NY, USA) containing 10% fetal bovine serum (FBS), penicillin and streptomycin (100 U/mL each). The cells were routinely incubated at a constant controlled temperature incubator (DHP-9162, Shanghai Jiecheng laboratory apparatus, Shanghai, China) at 37 °C with 5% CO_2, with the solution replaced at regular 2 day intervals. Upon cell confluence had reached 80%–90%, the cells were subcultured. Next, in order to select the most suitable cell line, the miR-194 expression was quantified in the third-generation cells.

2.6. Cell grouping and transfection

The cells were assigned into blank (without any transfection), NC (transfected with miR-194 NC sequence), miR-194 mimic (transfected with miR-194 mimic sequence), miR-194 inhibitor (transfected with miR-194 inhibitor sequence), siRNA-PRC1 (transfected with siRNA-PRC1 sequence) and miR-194 inhibitor + siRNA-PRC1 (transfected with miR-194 inhibitor and siRNA-PRC1 sequences) groups. Both Huh-7 and HepG2 cells at the logarithmic growth were inoculated in a 6-well plate (3×10^5 cells/well) 24 h before transfection. Then, cells were transfected when cell confluence had reached 70%. Notably, the transfection was performed in accordance with the instructions of the lipofectamine™ 2000 (11668-019, Invitrogen Inc., New York, California, USA). Specifically, 5 μL lipofectamine™ 2000 and 5 μL corresponding above-mentioned plasmids (20 μmol) of each group were added into 250 μL Opti-MEM® I medium (31985070, Guangzhou Bafly Biotechnology Co., Ltd., Guangzhou, China) and incubated for 5 min. The solution was mixed in a uniform fashion and permitted to stand for a 20-min period until the transfection reagent mixture had formed. The medium in the 6-well plate was removed using a pipette. The cells were then washed three times using an Opti-MEM® I medium in order to remove the serum. The prepared transfection reagent was added into the 6-well plates. The cells were cultured for 4 to 6 h and further incubated in medium containing serum. Following a 48 h period, the cells were collected for further experiments.

2.7. Dual luciferase reporter gene assay

The biological prediction website at microRNA.org was employed to ascertain whether PRC1 was the direct target gene of miR-194. Based on the binding sequence between 3′UTR of PRC1 mRNA and miR-194, the target and mutant sequences were designed, with the target sequence subsequently chemically synthesized. Both ends of the sequence were added with restriction site Xho I and Not I, with the synthesized fragment being cloned into the pUC57 vector. Following identification of the positive clones, recombinant plasmids were verified via DNA sequencing, which were then sub-cloned into psiCHECK-2 vector and transferred into Escherichia coli DH5α cells to amplify plasmids. The plasmids were extracted based on the instructions of Omega plasmid mini kit. The cells were then inoculated into a 6-well plate (2×10^5 cells/well). After the cells adhered to the well, the cells were transfected in accordance with the aforementioned procedures. The cells were collected following incubation for 48 h. Based on the instructions of the dual luciferase detection kit (GeneCopoeia Inc., Germantown, MD), the effects of miR-194 on the luciferase activity of PRC1 3′-UTR was examined. The fluorescence intensity was detected using a Glomax20/20 luminometer (Promega Corporation, Madison, WI, USA). The experiment in each group was repeated three times.

Table 1
Primer sequences for RT-qPCR.

Gene	Sequence
miR-194	F: 5′-GCCCGCTGTAACAGCAACTCCAT −3′ R: 5′-GTGCAGGGTCCGAGGT-3′
PRC1	F: 5′-CCTGTGCCTACTTTGCCTGA-3′ R: 5′-CGTGGCTAACACCAAGTCCA-3′ A
β-catenin	F: 5′-TGCCAAGTGGGTGGTATAGAGG-3′ R: 5′-CGCTGGGTATCCTGATGTGC-3
Tcf-4	F: 5′-CGAGGGTGATGAGAACCTGC-3′ R: 5′-CCCATGTGATTCGATGCGT-3′
Wnt3a	F: 5′-CAGGGTGAAGACATGCTGGTG-3′ R: 5′-CGAGGCGCTGTCGTACTTGT-3′
Wnt10b	F: 5′- CGGGTCTCCTGTTCCTGGCGTTG −3′ R: 5′- AGTCAGAGCGAAAGGCTGCAAAGGTC-3′
E-cadherin	F: 5′-TGCTGTTTCTGGTTTCTGTTGG-3′ R: 5′-CCTTCTCCGTATTCTCCTCCCT-3′
N-cadherin	F: 5′-CTCCTATGAGTGGAACAGGAACG-3′ R: 5′-TTGGATCAATGTCATAATCAAGTGCTGTA −3′
GSK3β	F: 5′-GTTGGTAGGAGCTTGGTGCT-3′ R: 5′-AGGTGAAAAGGCAAGGGGAC-3′
GAPDH	F: 5′-AGAAGGCTGGGGCTCATTTG-3′ R: 5′-AGGGGCCATACACAGTCTTC-3′
U6	F: 5′-GTGCTCCCTGCTTCGGCAGCACATATAC-3′ R: 5′-AAAAATATGGAACGCTTCACGAATTTG-3′

Notes: RT-qPCR, reverse transcription quantitative polymerase chain reaction; F: forward, R: reverse; miR-194, microRNA-194; PRC1, protein regulator of cytokinesis 1; Tcf-4, T cell factor-4; Wnt3a, Wingless-type MMTV integration site family member 3 a; Wnt10b, Wingless-type MMTV integration site family member 10b; GSK3β, Glycogen synthase kinase 3β; GAPDH, Glyceraldehyde 3-phosphate dehydrogenase.

2.8. Reverse transcription quantitative polymerase chain reaction (RT-qPCR)

Total RNA was extracted from tissues and cells respectively using the miRNeasy Mini Kit (217004, Qiagen company, Hilden, Germany). The designed primers of miR-194, PRC1, β-catenin, T-cell factor (Tcf)-4, Wnt3a, Wnt10b, E-cadherin, N-cadherin, glycogen synthase kinase 3 (GSK-3β), glyceraldehyde-3-phosphate dehydrogenase (GAPDH) and U6 were all synthesized by the Takara Inc. (Dalian, China) (Table 1). Next, RNA was reversely transcribed into complementary DNA (cDNA) in accordance with the instructions of the PrimeScript RT reagent kit (RR036A,Takara, Dalian, China). The reverse transcription system (10 μL) was listed as follows: reverse transcription reaction at 37 °C 3 times (15 min per time) and reverse transcriptase inactivation reaction at 85 °C for 5 s. Reaction liquid was extracted to precede fluorescent quantitative PCR based on the instructions of SYBR® Premix Ex TaqTM II reagent kit (RR820A, Takara, Dalian, China). The 50 μL reaction system consisted of 25 μL 2 × SYBR® Premix Ex TaqTM II, 2 μL PCR forward primers, 2 μL PCR reverse primers, l μL 50 × ROX Reference Dye, 4 μL DNA template and 16 μL ddH_2O. RT-qPCR detection was performed using the ABI7500 quantitative PCR instrument (7500, ABI Company, Oyster Bay, NY, USA) using the following reaction conditions: pre-denaturation at 95 °C for 30 s, 40 cycles of denaturation at 95 °C for 5 s, annealing and extension at 60 °C for 34 s. U6 was regarded as the internal control of the relative expression of miR-194. GAPDH was considered as the internal control for the relative expression of PRC1, β-catenin, Tcf-4, Wnt10b, Wnt3a, E-cadherin, N-cadherin and GSK3β. The experiment was repeated 3 times. The relative expression of target genes was calculated using

the $2^{-\Delta\Delta Ct}$ method: $\Delta\Delta Ct = \Delta Ct_{HCCgroup} - \triangle Ct_{normalgroup}$; $\Delta Ct = Ct_{(targetgene)} - Ct_{(internalcontrol)}$.

2.9. Western blot analysis

Following 48 h of transfection, total protein from fresh HCC tissues was extracted using the Radio-Immunoprecipitation assay (RIPA) kit (R0010, Beijing Solarbio Technology Co., Ltd., Beijing, China). The protein concentration was measured using the bicinchoninic acid (BCA) method. The protein was then transferred onto the nitrocellulose membrane by means of electrotransfer following electrophoretic separation using 10% sodium dodecyl sulfate polyacrylamide gel electrophoresis (SDS-PAGE). After blocking with 5% skimmed milk powder (dissolved by Tris-buffered saline [TBS]) at room temperature for 1 h, the membrane was incubated overnight at 4 °C with the addition of diluted primary antibodies rabbit-anti PRC1 (1: 1000, ab140033), β-catenin (1: 4000, ab6302), Tcf-4 (1: 1000, ab185736), Wnt3a (1: 1000, ab28472), Wnt10b (1: 2000, ab70816), E-cadherin (1: 500000, ab76319), N-cadherin (1: 1000, ab18203), GSK3β (1: 5000, ab32391) and p-GSK3β (1: 1000, ab75745). All these antibodies were purchased from the Abcam Inc. (Cambridge, MA, USA). Afterwards, the membrane was rinsed three times using a TBS + Tween 20 (TBST) (10 min per time), followed by incubation with HRP-labeled goat-anti-mouse IgG antibody (1: 3000, ab6721, Abcam Inc., Cambridge, MA, USA). Next, the proteins were visualized by enhanced chemiluminescence (ECL) reagent (WBKLS0500, Pierce, Rockford, IL, USA). After being developed in a dark place, the membrane was photographed and the results were observed.

2.10. 3-(4,5-dimethylthiazol-2-yl)-2,5-diphenyltetrazolium bromide (MTT) assay

Following a 48 h period of transfection, the cells were re-suspended and collected for cell counting purposes. The cells were then inoculated into a 96-well plate (4×10^3 cells/well, 200 μL per well) and cultured in an incubator. Each group was repeated in 6 wells. Three time points (24 h, 48 h and 72 h) were set for the following experiment. After 20 μL MTT solution was added into each well, the cells were further cultured at 37 °C for 4 h, and the culture was then terminated. After cautiously removing the culture supernatant in each well, cells in each well were added with 150 μL dimethyl sulfoxide (DMSO) and gently shaken on a horizontal table for 10 min to fully dissolve crystal. The optical density (OD) at 570 nm of each well was measured using a microplate reader (NYW-96 M, Peking Nuoya Wei Instrument Co., Ltd., Beijing, China). The experiment was repeated 3 times. The cell growth curve was plotted with the time points as the abscissa and the OD values as the ordinate.

2.11. Scratch test

Following 48 h of transfection, the cells were seeded into a 6-well plate. After cells adhered to the well, the cells were cultured into a serum-free Dulbecco's Modified Eagle's Medium (DMEM). When cell confluence reached 90%–100%, a 10 μL micropipette head was utilized to carefully create vertical scratches on the bottom of the 6 well-plate (5 to 6 scratches per well with the same width). The cells were then washed three times with PBS to remove the scratched cells. The 6-well plate was subsequently cultured in an incubator. At 0 and 24 h after scratching, several fields were randomly selected. An inverted microscope was applied to observe the migration distance in cell scratch area and then photographed. Each group was set with 3 duplicate wells and the experiment was repeated 3 times.

2.12. Transwell assay

The initial step for the Transwell assay was to transfer Matrigel, which was stored at −20 °C, to a separate location at 4 °C in order to thaw. The Matrigel was then diluted using serum-free DMEM at a ratio of 1: 2 on ice and uniformly mixed. About 20 μL of Matrigel was added dropwise on the membrane and incubated at 37 °C for 45 min and exposed to ultraviolet light for 45 min. Following 48 h of transfection, the cells were starved in a serum-free medium for 24 h, detached with trypsin, and re-suspended with serum-free DMEM following routine detachment. Following the detachment period, the apical chamber of the Transwell was added with 1.0 to 1.5×10^5 cells (cell volume <200 μL) and the basolateral chamber was added with 500 μL DMEM containing 10% FBS. The apical chamber of the Transwell was subsequently placed into the basolateral chamber. Due to the possibility of bubbles influencing the experiment results, extensive efforts were made in order to avoid the formation of bubbles between the medium and membrane. After a 24 h period, the apical chamber of the Transwell was removed and the cells on the membrane were removed using cotton swabs. After slight drying, the membrane was stained with 0.1% crystal violet for 15 min, washed gradually under running water, and photographed under a microscope. If the experiment permitted, the membrane was faded with 500 μL 33% acetic acid solution. Finally, the OD value was measured and statistically analyzed.

2.13. Tumor xenograft in nude mice

A total of 36 BALB/c nude mice (4 weeks old, weighing 14 to 16 g, half male and half female) were purchased from the Experimental Animal Center of Chinese Academy of Sciences (Shanghai, China). The selected HCC cells were then inoculated into a 24-well plate. When cell confluence reached 20%, lentivirus containing luciferase was added into the serum-free medium according to multiplicity of infection (MOI = 10). Following 12 h of transfection, the cells were further cultured in a serum medium for 48 h. The cells were harvested after screening with puromycin for 96 h in order to amplify and establish HCC cell lines stably expressing luciferase. A total of 1×10^4 HCC cells that stably expressing luciferase were plated into a 24-well plate, with fluorescein (final concentration at 150 ug/mL) added into each well. Cell luciferase intensity was detected using the Whole-Body Imaging System. A total of 36 mice were assigned into 12 groups (two cell lines, each cell line for the blank, NC, miR-194 mimic, miR-194 inhibitor, siRNA-PRC1 and miR-194 inhibitor + siRNA-PRC1 groups) with 3 mice per group. The nude mice were acclimatized for one week. The transfected cells were made into 4×10^7 cells/mL cell suspension for further use. The nude mice were intraperitoneally injected with pentobarbital sodium, and fixed on the operation table under a super clean sterile bench. Then mice were sterilized by iodine and covered with aseptic towels. The abdominal wall of the mice was cut open to expose the liver, and 25 μL of cell suspension (1×10^6) was injected under the liver capsule using a micro injector. The abdominal wall was then gradually sutured using 2 μL medical adhesive to seal the pinhole. The nude mice were continually observed until they had recovered from the effects of anesthesia. Following transplantation, the nude mice underwent bioluminescent living imaging once a week and were permitted with free access to food for 4 weeks. Before imaging, the nude mice were intraperitoneally injected with 0.1 mL 15 mg/mL fluorescein and granted freedom to move for 10 min. With anesthesia maintained with constant isoflurane, *in vivo* fluorescence imaging was performed under the Lumina II imaging system to observe the tumor growth of nude mice. After a 4 week period, the nude mice were euthanized. Liver tissues in addition to any potentially metastatic lymph node tissues were resected and fixed into 4% neutral formaldehyde overnight. The tissues were embed-

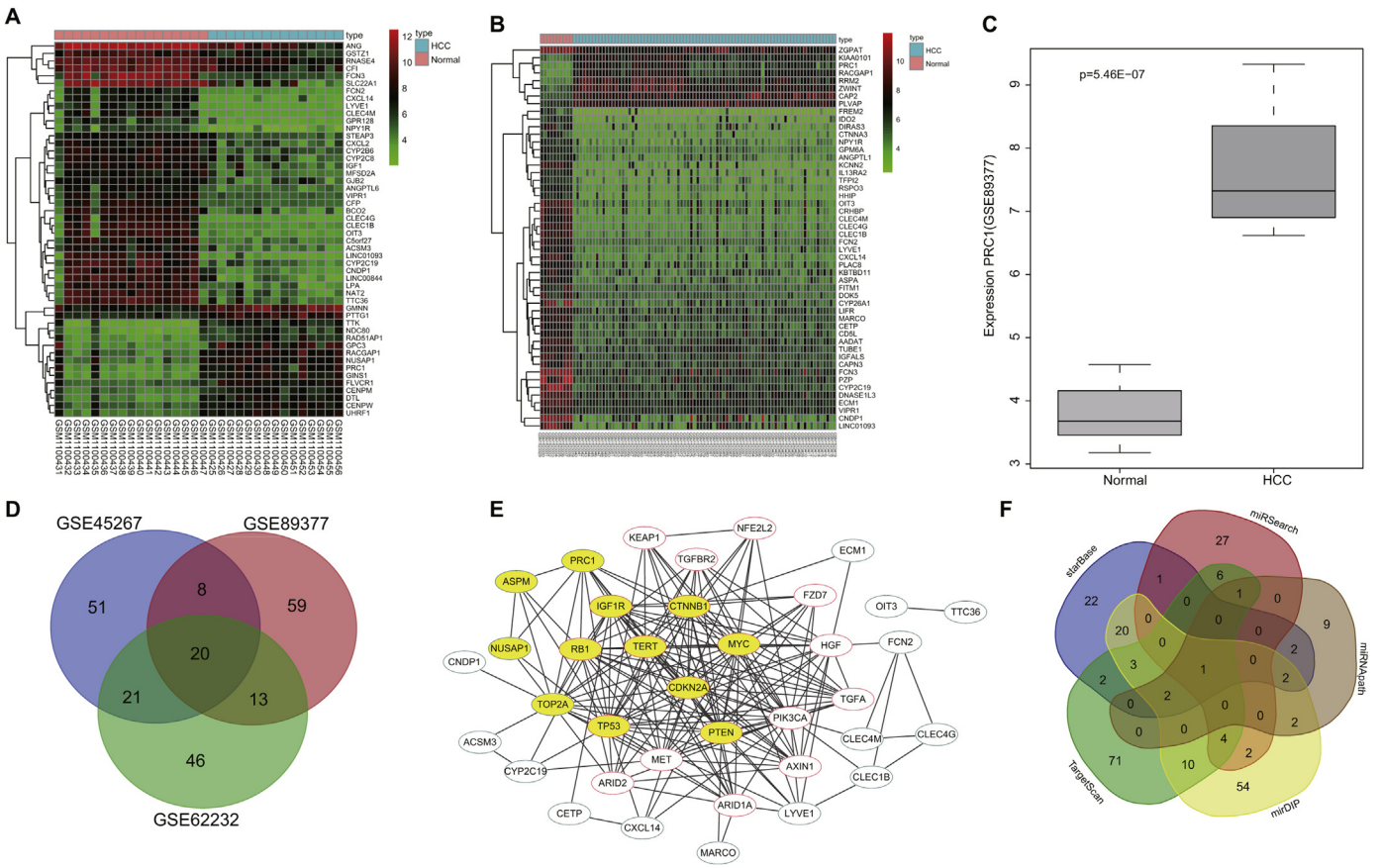

Fig. 1. Microarray-based analysis indicates that miR-194 regulates HCC through the Wnt/β-catenin signaling pathway by binding to PRC1. A and B, heat maps of DEGs in HCC expression profiles. X-axis represents sample number and Y-axis represents gene names, dendrogram in the left represents gene expression cluster, each cube represents the expression of a gene in a sample, upper right histogram is color gradation, C, the expression of PRC1 on HCC expression profile GSE89377. X-axis represents the sample type and Y-axis represents the expression of PRC1, box plot in the left represents PRC1 expression in the normal sample and box plot in the right represents PRC1 expression in the HCC samples, *p* value was on the top left corner. D, Venn analysis of the first 100 genes in 3 HCC expression profiles, 3 circles with different colors represent DEGs in 3 HCC expression profiles, cross region represents their interaction and the middle part is their intersection. E, protein interactive network, each ellipse represents a gene and lines connecting these ellipses represents interaction exists in two genes, periphery green ellipse represents HCC DEGs obtained from microarray analysis and periphery red ellipse represents HCC related genes obtained from the KEGG database, ellipse filled with yellow represents interactive genes with PRC1. F, predicted results on regulatory miRNA of PRC1, 5 irregular figures with different colors represent predicted results of 5 databases and the middle part represents their intersection. miR-194, microRNA-194; PRC1, protein regulator of cytokinesis 1; HCC, hepatocellular Carcinoma; KEGG, Kyoto Encyclopedia of Genes and Genomes; DEGs, differentially expressed genes.

ded with paraffin at an interval of 50 μm, cut into 10 sheets of 5 μm serial sections, which were then stained with hematoxylin and eosin (HE). The total number of metastasized tumors on each section was observed under a microscope with tumor volume measured accordingly.

2.14. Statistical analysis

All data analysis was performed using SPSS 21.0 software (IBM Corp. Armonk, NY, USA). Measurement data were presented as the mean ± standard deviation. The enumeration data were examined using chi–square test. Comparisons between HCC tissues and adjacent normal tissues were performed using a paired *t*-test. Besides, comparison between two groups was analyzed by independent sample *t*-test, while comparison among multiple groups was analyzed using one-way analysis of variance (ANOVA). $p < 0.05$ was considered to be statistically significant.

3. Results

3.1. MiR-194 plays a regulatory role in HCC through PRC1-mediated Wnt/β-catenin signaling pathway

HCC-related expression profiles GSE45267, GSE62232 and GSE89377 were retrieved from the GEO database. A total of 286, 230 and 425 DEGs were obtained respectively by differential expression analysis in the three expression profiles of the HCC samples and normal samples. The expression heat maps of 50 DEGs in GSE45267 and GSE62232 are depicted in Fig. 1 A–B. The expression of the candidate gene PRC1 in GSE89377 is illustrated in Fig. 1C. In order to further select HCC-related genes, the intersection of the top 100 DEGs from these three expression profiles was determined to construct a Venn histogram (Fig. 1 D), with 20 genes found to be located in the intersecting region. The "hepatocellular carcinoma" was also retrieved in the KEGG database and known HCC-related genes (H00048) were obtained. Association analysis of the DEGs in the intersection with known HCC-related genes in the KEGG database was performed after which the protein interactive network was constructed (Fig. 1 E). The results revealed that the majority of known genes in the KEGG database were located at the center of the protein interactive network. Among the 20 DEGs, TOP2A and PRC1 were located at a relatively central area and were observed to interact with most of the other known genes. Further information retrieval regarding these two genes implicated TOP2A in the development of HCC [22–24]. The effect of PRC1 on HCC at present has been insufficiently investigated. The analysis of the three HCC expression profiles revealed that the expression of PRC1 was noticeably up-regulated among the HCC samples (Fig. 1 A-C). Hence, PRC1 was selected as the subject of fol-

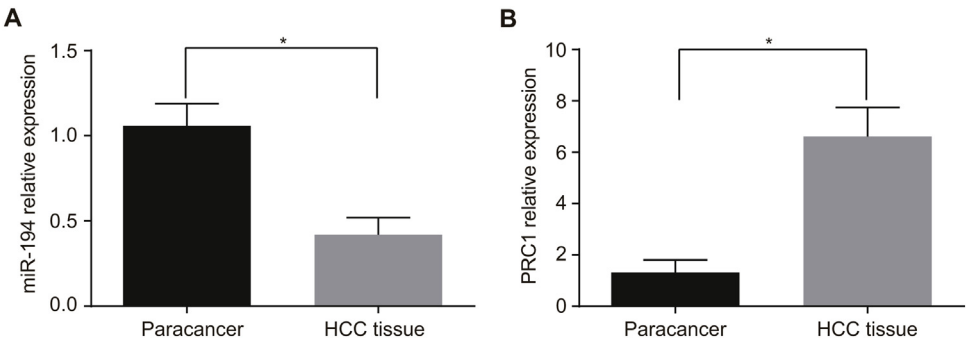

Fig. 2. HCC exhibits down-regulated miR-194 expression along with up-regulated PRC1 expression. * $p < 0.05$ compared with adjacent normal tissues. miR-194, microRNA-194; PRC1, protein regulator of cytokinesis 1; HCC, hepatocellular carcinoma.

lowing experiments. Recent investigations of HCC have indicated that the Wnt/β-catenin signaling pathway plays an important regulatory role in its development [25–27]. PRC1 has been revealed to affect tumor progression through the Wnt/β-catenin signaling pathway [28,29]. Collectively, the results obtained and the reports reviewed implied the effect of PRC1 on HCC, which was achieved through the Wnt/β-catenin signaling pathway. In order further elucidate the upstream regulatory mechanism of PCR1, StarBase and other databases were employed to predict the regulatory miRNAs of PRC1, and the intersection of the predicted results was obtained (Fig. 1 F). A large number of miRNAs were predicted in the mirDIP and TargetScan databases, while relatively few were identified from the remaining three databases. Therefore, the top 100 miRNAs from the predicted results in the mirDIP and TargetScan databases were selected for analysis. The results demonstrated that only one miRNA found in the intersection of the five databases, namely miR-194. These findings provided evidence that miR-194 might regulate HCC through the Wnt/β-catenin signaling pathway by targeting PRC1.

3.2. MiR-194 is decreased while PRC1 is increased in HCC

Statistical results from 228 HCC tissues and adjacent normal tissues demonstrated that the expression of miR-194 in HCC tissues was lower than that of the adjacent normal tissues while the expression of PRC1 was observed to be higher than those of the adjacent normal tissues in HCC (both $p < 0.05$) (Fig. 2). The expression of miR-194 and PRC1 was both noted to be associated with HBsAg, differentiation degree of tumors and TNM stage (all $p < 0.05$), while no significant difference was found in age and gender of the patients (both $p > 0.05$) (Table 2). The findings demonstrated that miR-194 was down-regulated while PRC1 was up-regulated in HCC.

3.3. HCC has a higher PRC1 positive expression

Immunohistochemistry was applied to detect the positive rate of PRC1 protein, the results of which (Fig. 3) demonstrated that PRC1 could be detected in both the cytoplasm (brown yellow) and nucleus (brown) of HCC cells. The positive rate of the PRC1 protein in adjacent normal tissues was 28.46 ± 3.02%, which was markedly lower than the 65.35 ± 6.36% detected in the HCC tissues ($p < 0.05$). Taken together, the aforementioned results revealed that HCC exhibited an elevated positive rate of PRC1 protein.

3.4. MiR-194 targets PRC1

The bioinformatics online software and a dual luciferase reporter gene assay were conducted to predict and verify the targeting relationship between miR-194 and PRC1. The results of online analysis software revealed that the PRC1 gene sequence and miR-194 sequence had specific binding sites, and PRC1 was shown to be a target gene of miR-194 (Fig. 4 A). The dual luciferase reporter gene assay indicated (Fig. 4 B) that when compared to that of the NC group, the wild type (Wt)-miR-194/PRC1 co-transfected group displayed diminished luciferase activity ($p < 0.05$), while no significant difference was observed in the mutant type (Mut)-miR-194/PRC1 co-transfected group ($p > 0.05$). These findings showed that miR-194 could specifically bind to PRC1.

Table 2
The expression of miR-194and PRC1 is associated with the progression of HCC.

Clinicopathological features	Case	miR-194	p	PRC1	p
Age (Years)			0.428		0.355
<51	115	0.42 ± 0.09		6.68 ± 1.12	
≥51	113	0.43 ± 0.10		6.54 ± 1.16	
Gender			0.428		0.742
Male	124	0.42 ± 0.09		6.59 ± 1.08	
Female	104	0.43 ± 0.10		6.64 ± 1.21	
HBsAg			<0.001		<0.001
Yes	135	0.38 ± 0.06		7.28 ± 0.86	
No	93	0.49 ± 0.09		5.64 ± 0.73	
Tumor differentiation			<0.001		<0.001
Low and middle differentiation	145	0.38 ± 0.04		7.24 ± 0.82	
High differentiation	83	0.51 ± 0.11		5.51 ± 0.68	
TNM stage			0.001		<0.001
I–II stage	158	0.46 ± 0.10		6.20 ± 0.99	
III–IV stage	70	0.42 ± 0.04		7.53 ± 0.89	

Notes: miR-194, microRNA-194; PRC1, protein regulator of cytokinesis 1; HCC, hepatocellular carcinoma; TNM, tumor-nodes-metastasis.

3.5. HCC cell lines HepG2 and Huh-7 show upregulated PRC1 expression

After determining that miR-194 targets PRC1, the next step was to analyze the PRC1 expression in the HCC cell lines. HCC cell lines with higher PRC1 expression were selected from HepG2, Hep 3B2.1-7, Huh-7 and Li-7 through RT-qPCR. The results revealed that PRC1 expression was largely varied among the HCC cell lines relative to human normal hepatocyte L02 (Supplementary Fig. 1). HepG2 and Huh-7 cell lines showed higher expression of PRC1 than Hep 3B2.1-7 and Li-7 cell lines (all $p < 0.05$). Therefore, HCC cell lines HepG2 and Huh-7 were selected for subsequent experiments.

3.6. Overexpressed miR-194 downregulates PRC1, inhibits EMT and inactivates the Wnt/β-Catenin signaling pathway

RT-qPCR was applied to measure the expression of miR-194 along with the mRNA expression of PRC1, β-catenin, Tcf-4, Wnt3a, Wnt10b, E-cadherin, N-cadherin and GSK3β in HCC cells. The results highlighted a similar trend regarding the Huh-7 and HepG2 cell lines (Supplementary Fig. 2 A-B). No significant difference

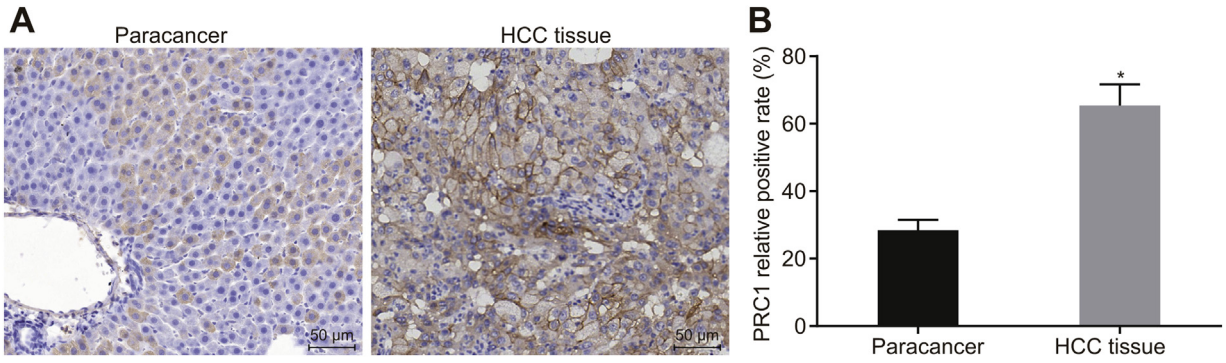

Fig. 3. HCC exhibits increased PRC1 positive expression rate. A, PRC1 expression in HCC tissues and adjacent normal tissues, which was detected through immunohistochemistry (×200). B, positive rate of PRC1 protein in HCC tissues and adjacent normal tissues. *, $p < 0.05$ compared with adjacent normal tissues; PRC1, protein regulator of cytokinesis 1; HCC, hepatocellular carcinoma.

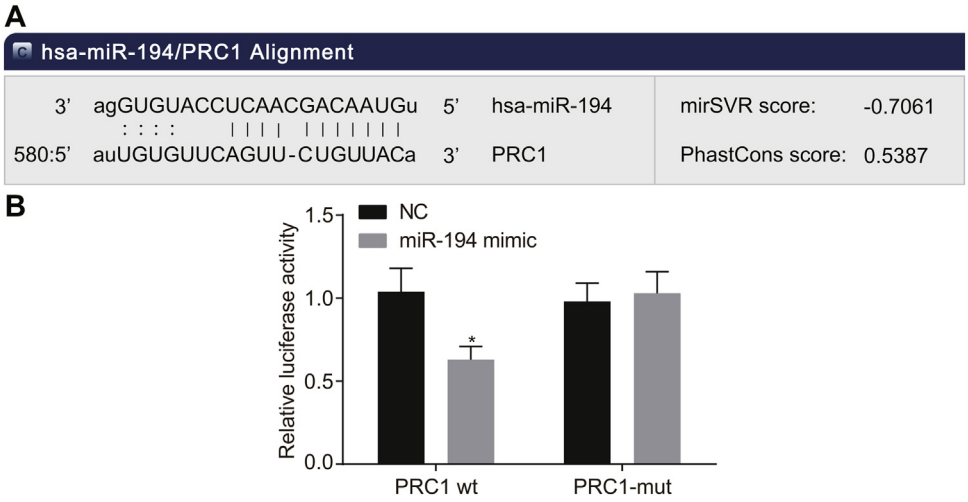

Fig. 4. PRC1 is a target gene of miR-194. A, predicted binding site of miR-194 on PRC1-3′UTR. B, luciferase activity of PRC1 wt and PRC1-mut detected by dual luciferase reporter gene assay. * $p < 0.05$ compared with the NC group. miR-194, microRNA-194; PRC1, protein regulator of cytokinesis 1; HCC, Hepatocellular Carcinoma; UTR, untranslated regions; NC, negative control; wt, wild type; mut, mutant type.

was detected in the blank and NC groups in the expression of above-mentioned factors (all $p > 0.05$). When compared to that of the blank and NC groups, the miR-194 mimic and siRNA-PRC1 groups exhibited significantly downregulated mRNA expression of PRC1, β-catenin, Tcf-4, Wnt3a, Wnt10b, N-cadherin and GSK3β, accompanied by increased mRNA expression of E-cadherin (all $p < 0.05$). Furthermore, the miR-194 mimic group exhibited an increase in miR-194 expression, ($p < 0.05$) while no obvious difference in regard to miR-194 was observed in the siRNA-PRC1 group ($p > 0.05$) when compared to that of the blank and NC groups. Relative to that of the blank and NC groups, the miR-194 inhibitor group showed elevated mRNA expression of PRC1, β-catenin, Tcf-4, Wnt3a, Wnt10b, N-cadherin and GSK3β, while mRNA expression of E-cadherin was shown to be significantly decreased (all $p < 0.05$). Besides, the miR-194 inhibitor + siRNA-PRC1 group demonstrated a drop in miR-194 expression ($p < 0.05$), and no notable change in the mRNA expression of PRC1, β-catenin, Tcf-4, Wnt3a, Wnt10b, E-cadherin, N-cadherin and GSK3β was detected (all $p > 0.05$).

Western blot analysis was subsequently performed in order to measure protein expression of PRC1, β-catenin, Tcf-4, Wnt3a, Wnt10b, E-cadherin, N-cadherin, GSK3β as well as the extent of GSK3β phosphorylation. The results obtained indicated there were similar trends in the protein expression of above-mentioned factors in the Huh-7 and HepG2 cell lines (Supplementary Fig. 3A–D). No statistical difference in regard to the protein expression of the above-mentioned factors was noted in the blank and NC groups (all $p > 0.05$). When compared to that of the blank and NC groups, the miR-194 mimic and siRNA-PRC1 groups exhibited a decrease in the protein expression of PRC1, β-catenin, Tcf-4, Wnt3a, Wnt10b, N-cadherin, and GSK3β as well as the extent of GSK3β phosphorylation, accompanied by elevated protein expression of E-cadherin (all $p < 0.05$). Furthermore, versus the blank and NC groups, the protein expression of PRC1, β-catenin, Tcf-4, Wnt3a, Wnt10b, N-cadherin, and GSK3β as well as the extent of GSK3β phosphorylation was all increased while that of E-cadherin was decreased in the miR-194 inhibitor group ($p < 0.05$). No significant difference was found in regard to the protein expression of PRC1, β-catenin, Tcf-4, Wnt3a, Wnt10b, E-cadherin, N-cadherin, and GSK3β as well as the extent of GSK3β phosphorylation in the miR-194 inhibitor + siRNA-PRC1 group (all $p > 0.05$). Taken together, a conclusion was reached suggesting that when miR-194 was upregulated, PRC1 was decreased, EMT was suppressed and the Wnt/β-catenin signaling pathway was inhibited.

3.7. Up-regulation of miR-194 or down-regulation of PRC1 inhibits cell proliferation in HCC

MTT assay was conducted in order to detect the viability of HCC cells. The results (Supplementary Fig. 4) revealed that Huh-7 and HepG2 cells had the same tendency. There was no obvious difference among the miR-194 inhibitor + siRNA-PRC1, blank group and NC group concerning cell viability (all $p > 0.05$). When com-

pared with the blank and NC groups, HCC cell viability was shown to decrease in the miR-194 mimic and siRNA-PRC1 groups but increase in the miR-194 inhibitor group (all $p < 0.05$). These results indicated that the up-regulation of miR-194 or down-regulation of PRC1 plays a significant role in decreasing cell proliferation in HCC.

3.8. Up-regulation of miR-194 or down-regulation of PRC1 reduces cell migration in HCC

A scratch test was applied in order to measure cell migration in HCC. Results indicated that Huh-7 and HepG2 cells had the same trend (Supplementary Fig. 5A-D). Cell migration did not differ greatly between the blank and NC groups ($p > 0.05$). Compared with the blank and NC groups, the miR-194 mimic and siRNA-PRC1 groups demonstrated reduced cell migration ability while the miR-194 inhibitor group exhibited a marked increase in cell migration ability (all $p < 0.05$). No significant difference was detected in regard to the cell migration ability in the miR-194 inhibitor + siRNA-PRC1 ($p > 0.05$). These findings demonstrated that overexpressed miR-194 or silenced PRC1 decreased cell migration in HCC.

3.9. Up-regulated miR-194 or down-regulated PRC1 represses cell invasion in HCC

Transwell assay was performed in order to determine cell invasion in HCC. The results obtained highlighted a similar trend between the Huh-7 and HepG2 cells (Supplementary Fig. 6 A–D). No significant difference was observed in the cell invasion ability between the blank and NC groups ($p > 0.05$). When compared to that of the blank and NC groups, the miR-194 mimic and siRNA-PRC1 groups displayed reduced cell invasion ability, while the miR-194 inhibitor group exhibited notably elevated cell invasion ability (all $p < 0.05$). No significant difference was detected in the cell invasion ability in the miR-194 inhibitor + siRNA-PRC1 group in comparison with the blank and NC groups (both $p > 0.05$). The results indicated that miR-194 up-regulation or PRC1 down-regulation contributed to decreased cell invasion ability in HCC.

3.10. Up-regulated miR-194 or silenced PRC1 suppresses tumor growth of HCC in vivo

The tumor xenograft was induced in nude mice in order to assess tumor growth of HCC, the results of which highlighted a similar trend regarding the Huh-7 cells and HepG2 cells (Supplementary Fig. 7A–D). Compared with the blank and NC groups, the miR-194 mimic and siRNA-PRC1 groups exhibited reduced tumor volume as well as a decline in the number of metastatic lymph nodes which was accompanied by a slow growth rate (all $p < 0.05$), while the miR-194 inhibitor group exhibited an increase in tumor volume along with an elevated number of metastatic lymph nodes, accompanied with a rapid growth rare (all $p < 0.05$). No significant difference was found in the miR-194 inhibitor + siRNA-PRC1 group in comparison with the blank and NC groups ($p > 0.05$). The results illustrated that tumor growth was reduced in HCC in response to miR-194 elevation or PRC1 reduction.

4. Discussion

HCC remains one of the foremost leading causes of cancer related deaths worldwide, accompanied with a poor prognosis in both developed and developing countries, with its etiology and occurrence often linked with the rising incidence of hepatitis B and C infection [4]. Although widely viewed as an auxiliary treatment approach, liver surgical excision and diagnosis at an early stage has achieved some progress, however HCC patients still suffer from a worse prognosis and run the high risk of postoperative recurrence due to high cell invasion and migration [30]. Accumulating evidence has highlighted the abnormal expression of certain miRNAs, which play a regulatory role in a variety of processes of cancer development, such as tumor formation, cell migration and proliferation, by regulating the expression of oncogenes or cancer suppressors [31]. Thus, the current study set out to investigate the role of miR-194 in HCC. The data obtained from the present study revealed that up-regulation of miR-194 was shown to inhibit EMT, cell invasion and migration ability through downregulating PRC1 and inactivating the Wnt/β-catenin signaling pathway in HCC.

The key observations of the study revealed that miR-194 was poorly expressed, while PRC1 was highly expressed in HCC. Existing studies have established the aberrant expression of miRNAs in HCC, for instance, miR-127 has been reported to exhibit decreased levels of expression in HCC cell lines and tissues [32]. Furthermore, a recent study has also suggested the diminished miR-448 expression in HCC, the loss of which leads to enhanced cell invasion and EMT through modulating ROCK2 in HCC [33]. Consistent with our findings, the down-regulation of miR-194 has been found in gastric cancer tissues and its knockdown has been directly linked with tumor node metastasis, tumor invasion [34]. At the same time, a recent study has revealed that PRC1 is elevated in gastric cancer and its up-regulation promotes tumor growth, cell invasion, migration and proliferation [13]. The overexpression of PRC1 has been demonstrated to inhibit 5-FU-induced G2/M phase arrest, decrease 5-FU-induced apoptosis and elevate chemical resistance in HCC cells, which ultimately leads to a poor survival rate of patients with HCC [12]. These results were consistent with the findings of the current study, whereby miR-194 was noted to be down-regulated while PRC1 was up-regulated in HCC.

Furthermore, the obtained data suggested the overexpression of miR-194 and the silencing of PRC1 resulted in the reduced expression of PRC1, β-catenin, Tcf-4, Wnt3a, Wnt10b, N-cadherin and GSK3β, accompanied by increased E-cadherin expression, indicating that miR-194 elevation and PRC1 silencing could inhibit EMT and inactivate the Wnt/β-catenin signaling pathway. EMT, a significant part in tumor development, has been reported to undergo alterations during the interaction between cell and matrix, cell and cell, cell activity as well as anchorage that permits invasion and migration of cells [6]. It has been indicated that miR-194 acts to restrain EMT in endometrial cancer cells via binding to carcinogene BMI-1 [35]. A recent study has indicated similar situation that miR-26a restrains EMT by suppressing the enhancer of zeste homolog 2 in HCC cells [36]. In addition, the overexpression of miR-200a contributes to reduced tumor progression and EMT through inactivating the Wnt/β-catenin signaling pathway and elevating E-cadherin via binding to ZEB1 and ZEB2 in gastric adenocarcinoma [37]. These findings were in consistence with the results of the current study, whereby miR-194 restrained EMT, cell proliferation, invasion and migration by inhibiting PRC1 expression and suppressing the Wnt/β-catenin signaling pathway in HCC.

Furthermore, up-regulated miR-194 or silenced PRC1 suppresses tumor growth and lymph node metastasis of HCC *in vivo*. PRC1 knockdown has been proven to inhibit invasion and proliferation in lung cancer cells and suppress tumor formation by cutting off cytokinesis [38]. Abnormally activated Wnt/β-catenin signaling pathway has been found in various cancers and its inactivation inhibits stem cell formation, tumor cell development and viability in osteosarcoma [39]. Furthermore, cell invasion and migration are restrained by miR-214-5p through binding to Wiskott-Aldrich Syndrome Like in HCC cells [40]. All these findings were in line with our data which demonstrated that miR-194 inhibited tumor progression through downregulating of PRC1 and inactivation of the Wnt/β-catenin signaling pathway in HCC.

In conclusion, the key findings of this study revealed that miR-194 repressed EMT, cell proliferation, invasion and migration

through PRC1 downregulation and inactivation of the Wnt/β-catenin signaling pathway in HCC (Supplementary Fig. 8). These findings may shed new lights for developing possible strategies in the HCC treatment. It is expected that further studies concerning the mechanism of miR-194, PRC1 and the Wnt/β-catenin signaling pathway in other cancer types will be conducted in the future. Whether the mechanism involved with miR-194 affecting EMT of HCC via the Wnt/β-Catenin signaling pathway is only associated with PRC1 or associated with both PRC1 and PRC1-mediated BMI-1 would be further explored.

Conflict of interest

None declared.

Acknowledgement

We thank the reviewers for critical comments.

Appendix A. Supplementary data

Supplementary data associated with this article can be found, in the online version, at https://doi.org/10.1016/j.dld.2019.02.012.

References

[1] Huang JT, Liu SM, Ma H, Yang Y, Zhang X, Sun H, et al. Systematic review and meta-analysis: circulating miRNAs for diagnosis of hepatocellular carcinoma. J Cell Physiol 2016;231:328–35.
[2] Liu Y, Chai Y, Zhang J, Tang J. A function variant at miR-501 alters susceptibility to hepatocellular carcinoma in a Chinese Han population. Cell Physiol Biochem 2016;38:2500–8.
[3] Tang H, Zhang J, Yu Z, Ye L, Li K, Ding F, et al. Mir-452-3p: a potential tumor promoter that targets the CPEB3/EGFR axis in human hepatocellular carcinoma. Technol Cancer Res Treat 2017;16:1136–49.
[4] Zhao L, Zhang Y, Zhang Y. Long noncoding RNA CASC2 regulates hepatocellular carcinoma cell oncogenesis through miR-362-5p/Nf-kappaB axis. J Cell Physiol 2018;233:6661–70.
[5] Suzhi Z, Liang T, Yuexia P, Lucy L, Xiaoting H, Yuan Z, et al. Gap junctions enhance the antiproliferative effect of MicroRNA-124-3p in glioblastoma cells. J Cell Physiol 2015;230:2476–88.
[6] Bacigalupo ML, Manzi M, Espelt MV, Gentilini LD, Compagno D, Laderach DJ, et al. Galectin-1 triggers epithelial-mesenchymal transition in human hepatocellular carcinoma cells. J Cell Physiol 2015;230:1298–309.
[7] Zhang JW, Li Y, Zeng XC, Zhang T, Fu BS, Yi HM, et al. miR-630 overexpression in hepatocellular carcinoma tissues is positively correlated with alpha-fetoprotein. Med Sci Monit 2015;21:667–73.
[8] Xu H, Zhu J, Hu C, Song H, Li YY. Inhibition of microRNA-181a may suppress proliferation and invasion and promote apoptosis of cervical cancer cells through the PTEN/Akt/FOXO1 pathway. J Physiol Biochem 2016;72:721–32.
[9] Salta E, De Strooper B. microRNA-132: a key noncoding RNA operating in the cellular phase of Alzheimer's disease. FASEB J 2017;31:424–33.
[10] Sun JJ, Chen GY, Xie ZT. MicroRNA-361-5p inhibits cancer cell growth by targeting CXCR6 in hepatocellular carcinoma. Cell Physiol Biochem 2016;38:777–85.
[11] Meng Z, Fu X, Chen X, Zeng S, Tian Y, Jove R, et al. miR-194 is a marker of hepatic epithelial cells and suppresses metastasis of liver cancer cells in mice. Hepatology 2010;52:2148–57.
[12] Wang Y, Shi F, Xing GH, Xie P, Zhao N, Yin YF, et al. Protein regulator of cytokinesis PRC1 confers chemoresistance and predicts an unfavorable postoperative survival of hepatocellular carcinoma patients. J Cancer 2017;8:801–8.
[13] Zhang B, Shi X, Xu G, Kang W, Zhang W, Zhang S, et al. Elevated PRC1 in gastric carcinoma exerts oncogenic function and is targeted by piperlongumine in a p53-dependent manner. J Cell Mol Med 2017;21:1329–41.
[14] Chen J, Rajasekaran M, Xia H, Zhang XQ, Kong SN, Sekar K, et al. The microtubule-associated protein PRC1 promotes early recurrence of hepatocellular carcinoma in association with the Wnt/beta-catenin signalling pathway. Gut 2016;65:1522–34.
[15] Fan D, Ren B, Yang X, Liu J, Zhang Z. Upregulation of miR-501-5p activates the wnt/beta-catenin signaling pathway and enhances stem cell-like phenotype in gastric cancer. J Exp Clin Cancer Res 2016;35:177.
[16] Vilchez V, Turcios L, Marti F, Gedaly R. Targeting Wnt/beta-catenin pathway in hepatocellular carcinoma treatment. World J Gastroenterol 2016;22:823–32.
[17] Dahmani R, Just PA, Perret C. The Wnt/beta-catenin pathway as a therapeutic target in human hepatocellular carcinoma. Clin Res Hepatol Gastroenterol 2011;35:709–13.
[18] Huynh TT, Rao YK, Lee WH, Chen HA, Le TD, Tzeng DT, et al. Destruxin B inhibits hepatocellular carcinoma cell growth through modulation of the Wnt/beta-catenin signaling pathway and epithelial-mesenchymal transition. Toxicol In Vitro 2014;28:552–61.
[19] Lu Y, Li N, Gao L, Xu YJ, Huang C, Yu K, et al. Acetylcarnitine is a candidate diagnostic and prognostic biomarker of hepatocellular carcinoma. Cancer Res 2016;76:2912–20.
[20] Xie D, Yuan P, Wang D, Jin H, Chen H. Expression and prognostic significance of miR-375 and miR-221 in liver cancer. Oncol Lett 2017;14:2305–9.
[21] Zhong H, De Marzo AM, Laughner E, Lim M, Hilton DA, Zagzag D, et al. Overexpression of hypoxia-inducible factor 1alpha in common human cancers and their metastases. Cancer Res 1999;59:5830–5.
[22] Perng DS, Tsai YH, Cherng J, Wang JS, Chou KS, Shih CW, et al. Discovery of a novel anticancer agent with both anti-topoisomerase I and II activities in hepatocellular carcinoma SK-Hep-1 cells in vitro and in vivo: cinnamomum verum component 2-methoxycinnamaldehyde. Drug Des Dev Ther 2016;10:141–53.
[23] Panvichian R, Tantiwetrueangdet A, Angkathunyakul N, Leelaudomlipi S. TOP2A amplification and overexpression in hepatocellular carcinoma tissues. Biomed Res Int 2015;2015:381602.
[24] Wong N, Yeo W, Wong WL, Wong NL, Chan KY, Mo FK, et al. TOP2A overexpression in hepatocellular carcinoma correlates with early age onset, shorter patients survival and chemoresistance. Int J Cancer 2009;124:644–52.
[25] Wang H, Ma P, Liu P, Chen B, Liu Z. Small nucleolar RNA U2_19 promotes hepatocellular carcinoma progression by regulating Wnt/beta-catenin signaling. Biochem Biophys Res Commun 2018;500:351–6.
[26] Cui H, Song R, Wu J, Wang W, Chen X, Yin J. MicroRNA-337 regulates the PI3K/AKT and Wnt/beta-catenin signaling pathways to inhibit hepatocellular carcinoma progression by targeting high-mobility group AT-hook 2. Am J Cancer Res 2018;8:405–21.
[27] Jia P, Wei G, Zhou C, Gao Q, Wu YH, Sun XJ, et al. Upregulation of MiR-212 inhibits migration and tumorigenicity and inactivates Wnt/beta-catenin signaling in human hepatocellular carcinoma. Technol Cancer Res Treat 2018;17, 1533034618765221.
[28] Zhan P, Zhang B, Xi GM, Wu Y, Liu HB, Liu YF, et al. PRC1 contributes to tumorigenesis of lung adenocarcinoma in association with the Wnt/beta-catenin signaling pathway. Mol Cancer 2017;16:108.
[29] Hanselmann S, Wolter P, Malkmus J, Gaubatz S. The microtubule-associated protein PRC1 is a potential therapeutic target for lung cancer. Oncotarget 2018;9:4985–97.
[30] Yang F, Lv L, Zhang K, Cai Q, Liu J, Jiang Y. Elevated FOXC2 expression promotes invasion of HCC cell lines and is associated with poor prognosis in hepatocellular carcinoma. Cell Physiol Biochem 2017;44:99–109.
[31] Gao F, Sun X, Wang L, Tang S, Yan C. Downregulation of MicroRNA-145 caused by hepatitis B virus X protein promotes expression of CUL5 and contributes to pathogenesis of hepatitis B virus-associated hepatocellular carcinoma. Cell Physiol Biochem 2015;37:1547–59.
[32] Zhou J, Lu S, Yang S, Chen H, Shi H, Miao M, et al. MicroRNA-127 post-transcriptionally downregulates Sept7 and suppresses cell growth in hepatocellular carcinoma cells. Cell Physiol Biochem 2014;33:1537–46.
[33] Zhu H, Zhou X, Ma C, Chang H, Li H, Liu F, et al. Low expression of miR-448 Induces EMT and promotes invasion by regulating ROCK2 in hepatocellular carcinoma. Cell Physiol Biochem 2015;36:487–98.
[34] Chen X, Wang Y, Zang W, Du Y, Li M, Zhao G. miR-194 targets RBX1 gene to modulate proliferation and migration of gastric cancer cells. Tumour Biol 2015;36:2393–401.
[35] Dong P, Kaneuchi M, Watari H, Hamada J, Sudo S, Ju J, et al. MicroRNA-194 inhibits epithelial to mesenchymal transition of endometrial cancer cells by targeting oncogene BMI-1. Mol Cancer 2011;10:99.
[36] Ma DN, Chai ZT, Zhu XD, Zhang N, Zhan DH, Ye BG, et al. MicroRNA-26a suppresses epithelial-mesenchymal transition in human hepatocellular carcinoma by repressing enhancer of zeste homolog 2. J Hematol Oncol 2016;9:1.
[37] Cong N, Du P, Zhang A, Shen F, Su J, Pu P, et al. Downregulated microRNA-200a promotes EMT and tumor growth through the wnt/beta-catenin pathway by targeting the E-cadherin repressors ZEB1/ZEB2 in gastric adenocarcinoma. Oncol Rep 2013;29:1579–87.
[38] Zhan P, Xi GM, Liu HB, Liu YF, Xu WJ, Zhu Q, et al. Protein regulator of cytokinesis-1 expression: prognostic value in lung squamous cell carcinoma patients. J Thorac Dis 2017;9:2054–60.
[39] Dai G, Zheng D, Wang Q, Yang J, Liu G, Song Q, et al. Baicalein inhibits progression of osteosarcoma cells through inactivation of the Wnt/beta-catenin signaling pathway. Oncotarget 2017;8:86098–116.
[40] Li H, Wang H, Ren Z. MicroRNA-214-5p inhibits the invasion and migration of hepatocellular carcinoma cells by targeting Wiskott–Aldrich syndrome like. Cell Physiol Biochem 2018;46:757–64.